JOURNAL OF SYNCHROTRON RADIATION

ISSN 1600-5775

Received 8 April 2019
Accepted 30 May 2019

Edited by S. Svensson, Uppsala University, Sweden

Keywords: soft X-ray and vacuum ultraviolet; intrinsic aberrations; extrinsic aberrations; synchrotron optics; optical design.

Supporting information: this article has supporting information at journals.iucr.org/s

Method of calculating the aberrations of soft X-ray and vacuum ultraviolet optical systems

Yiqing Cao,[a,b]* Zhijuan Shen[a,b] and Zhixia Zheng[a,b]

[a]School of Mechanical and Electrical Engineering, Putian University, Putian, Fujian 351100, People's Republic of China, and [b]Fujian Laser Precision Machining Engineering Technology Research Center, Putian, Fujian 351100, People's Republic of China. *Correspondence e-mail: caoyiqing1987@163.com

Based on the the third-order aberration theory of plane-symmetric optical systems, this paper studies the effect on aberrations of the second-order accuracy of aperture-ray coordinates and the extrinsic aberrations of this kind of optical system; their calculation expressions are derived. The resultant aberration expressions are then applied to calculate the aberrations of two design examples of soft X-ray and vacuum ultraviolet (XUV) optical systems; images are compared with ray-tracing results using *SHADOW* software to validate the aberration expressions. The study shows that the accuracy of the aberration expressions is satisfactory.

1. Introduction

Soft X-ray and vacuum ultraviolet (XUV) optical systems are widely used with synchrotron radiation, X-ray microscopy, *etc.* (Owen *et al.*, 2016; Yang *et al.*, 2016; Underwood & Koch, 1997; Shealy *et al.*, 1995). The aberration analysis method is key to the optical system design in order to gain sufficiently high optical transmission in XUV optical systems, and researchers need to adopt a scheme where grazing-incidence rays impinge on the optical surface. Consequently, the shape of the wavefront will deviate significantly from spherical, and the focusing geometry of a light beam in the meridional plane will differ from that in the sagittal plane, and thus result in the imaging performance of a plane-symmetric optical system (Cao & Lu, 2017).

Many aberration analysis methods have been developed for plane-symmetric optical systems; for example, the light-path function (LPF) (Beulter, 1945; Noda *et al.*, 1974), analytic formulas of the ray-tracing spot diagram (SD) (Namioka *et al.*, 1994; Masui & Namioka, 1999), Lie optics (Goto & Kurosaki, 1993; Palmer *et al.*, 1998*a*,*b*) and wavefront aberration (WFA) (Chrisp, 1983; Lu, 2008). Lu (2008) adopted a toroidal surface as a reference wavefront to develop the third-order aberration theory of plane-symmetric optical systems based on the WFA method. The aberration theory was applicable to the aberrations analysis of XUV optical systems of mirrors or gratings of different surface types, but it adopted a linear approximation of the aperture-ray coordinates and only considered intrinsic aberrations of multi-element optical systems.

According to Gaussian optics, aperture-ray coordinates are usually approximated linearly in an axially symmetric multi-element optical system. In a plane-symmetric optical system, however, the light beam often impinges on the optical surface at oblique incidence, or even extremely grazing incidence. This usually causes serious aberrations, which will then cause the aperture ray to strongly deviate from the Gaussian optics. In

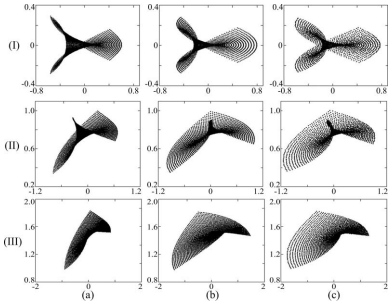

© 2019 International Union of Crystallography

addition, the aperture-ray coordinates of the optical surface will be modified by the aberrations of its preceding optical surface (*i.e.* extrinsic aberrations). Therefore, for an XUV optical system with a small meridional curvature radius of an optical surface or a large field angle of a point source, the calculation accuracy of the third-order aberration theory of plane-symmetric optical systems will have a significant error (Lu, 2008). We also need to consider the effects on the aberration due to the second-order accuracy of the aperture-ray coordinates and the extrinsic aberrations. Lu & Lin (2010) combined the WFA and SD methods to derive the aberration expressions of the wave-aberration form of double-element systems with the nonlinear accuracy of aperture-ray coordinates; however, it is not an analytic analysis method and is not suitable for multi-element optical systems. In this paper, we propose an analytical analysis method for the effect on the aberrations of the second-order accuracy of the aperture-ray coordinates and extrinsic aberrations of XUV multi-element optical systems.

In Sections 2 and 3 we introduce the definition and the third-order aberration theory of plane-symmetric optical systems (Lu, 2008), respectively, while in Section 4 the relation of aperture-ray coordinates between adjacent optical surfaces is fitted with a second-order polynomial, and, for the XUV optical system, we study the variation of the aperture-ray coordinates on the optical surface of the latter optical element due to the aberrations produced by its preceding optical element. In Section 5 we use the resultant aberrations formulae to calculate the imaging of two design examples of XUV optical systems, and the calculation results are validated with the ray-tracing program *SHADOW* (Sanchez del Rio, 2011).

2. Definition of plane-symmetric optical systems

Fig. 1 shows a plane-symmetric optical system with an off-plane object point S_0 (Lu, 2008). The optical surface is symmetrical with respect to the plane $\chi O z'$, where O is the vertex of the optical surface. O_0OO_1, lying in the symmetry plane, is defined as the base ray, whose angles of incidence and reflection are α and β, respectively, and their sign will be positive if rotation from the z'-axis to the ray is counterclockwise. The ray $S_0\overline{P}S_1$, emitted from source S_0 and passing through the center of the entrance pupil, is the principle ray; it intersects the optical surface at $\overline{P}$, which is stipulated to be the origin of the pupil coordinates system xyz. u and u' are the sagittal field angle in the object space and image space, respectively.

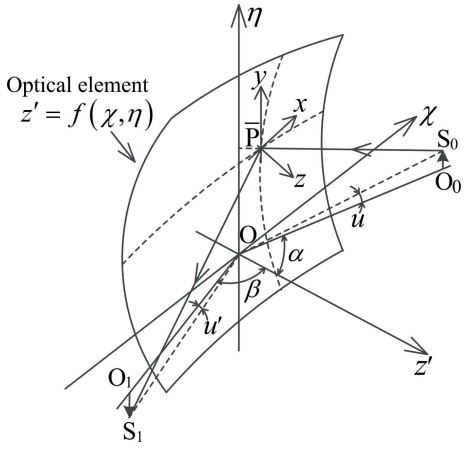

Figure 1
Optical scheme of a plane-symmetric optical system.

The general form of a plane-symmetric surface can be expressed in the vertex coordinate system of $\chi\eta z'$ by the equation (Lu & Cao, 2017)

$$z' = \sum_{i=0}^{\infty}\sum_{j=0}^{\infty} c_{i,j}\,\chi^i\,\eta^j, \qquad c_{0,0} = c_{1,0} = 0, \qquad j = \text{even}. \tag{1}$$

For the third-order aberration theory of plane-symmetric optical systems, the power series needs to be kept up to the fourth order; thus the figure equation is denoted by

$$z' = c_{2,0}\,\chi^2 + c_{0,2}\,\eta^2 + c_{3,0}\,\chi^3 + c_{1,2}\,\chi\,\eta^2 + c_{4,0}\,\chi^4 + c_{2,2}\,\chi^2\,\eta^2 + c_{0,4}\,\eta^4, \tag{2}$$

where the coefficient $c_{i,j}$ has been given for toroid, ellipsoid and paraboloid by Peatman (1997). For a toroidal surface, $c_{i,j}$ is as follows,

$$c_{2,0} = \frac{1}{2R}, \quad c_{0,2} = \frac{1}{2\rho}, \quad c_{3,0} = 0, \quad c_{1,2} = 0, \quad c_{4,0} = \frac{1}{8R^3}, \quad c_{0,4} = \frac{1}{8\rho^3}, \quad c_{2,2} = \frac{1}{4R^2\rho}, \tag{3}$$

where R and ρ are the major and minor curvature radii of the toroid. If $R = \rho$, equation (2) becomes a spherical equation, and, if R or ρ tend to infinity, then it becomes a cylindrical equation.

3. Third-order aberration theory of a multi-element plane-symmetric optical system

The wave aberration is derived from the light-path function; however, the groove function of a grating will also contribute to the wave aberration. The groove function $n = n(\chi, \eta)$ for holographic and mechanically ruled gratings is represented by (Cao & Lu, 2017)

$$n = \frac{\chi}{\sigma} + \frac{\Gamma}{\sigma}\left(\frac{n_{20}}{2}\chi^2 + \frac{n_{02}}{2}\eta^2 + \frac{n_{30}}{2}\chi^3 + \frac{n_{12}}{2}\chi\eta^2 + \frac{n_{40}}{8}\chi^4 + \frac{n_{22}}{4}\chi^2\eta^2 + \frac{n_{04}}{8}\eta^4 + \ldots\right), \tag{4}$$

where σ is the groove spacing of the grating at the vertex, and Γ and n_{ij} are given by equations (20)–(22) of Namioka *et al.* (1994). The wave aberration of a plane-symmetric optical system is represented by

$$W = \sum_{ijk}^{4} w_{ijk}\,x^i\,y^j\,u^k \qquad (i + j + k \le 4). \tag{5}$$

The wave-aberration coefficients w_{ijk} are given by

$$w_{ijk} = M_{ijk}(\alpha, r_m, r_s, l_s) + (-1)^k M_{ijk}(\beta, r'_m, r'_s, l'_s) + \Lambda N_{ijk}, \tag{6}$$

where x, y are the aperture-ray coordinates on the optical surface; $M_{ijk}(\alpha, r_m, r_s, l_s)$ are the wave-aberration coefficients of the object pencil and are listed in Appendix A of Lu & Zhu (2012); the parameters r_m, r_s, r'_m, r'_s represent the meridional and sagittal focal distances in the object and image space; l and l' are the parameters representing the position of the entrance and exit pupil; their expressions as well as N_{ijk} are given by Lu (2008) and $\Lambda = (m\lambda/\sigma)\Gamma$.

Similar to Gaussian optics, the first- and second-order wave-aberration should be zero to define the aberrations of plane-symmetric optical systems. The parameters α, β, l, l', r_m, r_s, r'_m, r'_s are determined by equations (4)–(7) of Cao & Lu (2017). Therefore, the imaging aberration is contributed by the remaining third- to fourth-order wave aberrations (Lu, 2008),

$$\begin{aligned} W = {} & w_{300}x^3 + w_{120}xy^2 + w_{400}x^4 + w_{220}x^2y^2 + w_{040}y^4 \\ & + w_{102}xu^2 + w_{013}yu^3 + w_{202}x^2u^2 + w_{022}y^2u^2 \\ & + w_{111}xyu + w_{031}y^3u + w_{211}x^2yu. \end{aligned} \tag{7}$$

For multi-element optical systems, the total wave aberration is the sum of the contribution from every optical element. Therefore, for an optical system of g elements the wave aberration is formulated as

$$\begin{aligned} W &= W_{(1)} + W_{(2)} + \ldots W_{(g)} \\ &= \sum_{n=1}^{g} \sum_{ijk}^{4} W_{ijk(n)}\, x_n^i\, y_n^j\, u_n^k \qquad (i+j+k \le 4). \end{aligned} \tag{8}$$

If the relation of the aperture-ray coordinates and the field angle between adjacent optical surfaces adopts the linear approximation,

$$x_i = A_i\, x_{i+1}, \quad y_i = -B_i\, y_{i+1}, \quad u_i = -(1/B_i)\, u_{i+1}, \tag{9}$$

where $A_i = r'_{m(i)} \cos\alpha_{i+1}/[r_{m(i+1)} \cos\beta_i]$ and $B_i = r'_{s(i)}/r_{s(i+1)}$.

For an XUV optical system with a small meridional curvature radius of the optical surface or a large field angle of a point source, the linear approximation is unsatisfactory; we will discuss the modification of the wave aberration using a second-order polynomial to fit the above relation in Section 4.

In the third-order aberration theory of plane-symmetric optical systems, the aperture-ray coordinates and the field angle on the final optical surface are usually assumed to be the reference ones of the optical systems. With the transfer equation (9), the wave aberration of equation (8) can be transformed into

$$\begin{aligned} W &= \sum_{ijk}^{4} W_{ijk}^T\, x_g^i\, y_g^j\, u_g^k, \\ W_{ijk}^T &= \sum_{n=1}^{g-1} W_{ijk(n)}\, A_{n|g}^i\, B_{n|g}^{j-k} + W_{ijk(g)}, \end{aligned} \tag{10}$$

where W_{ijk}^T is the wave-aberration coefficient with the linear approximation of the multi-element optical systems; and the coefficients of transformation with the linear approximation of the aperture-ray coordinates, $A_{n|g}$ and $B_{n|g}$, are calculated by

$$\begin{aligned} A_{n|g} &= \frac{r'_{m(n)} r'_{m(n+1)} \cdots r'_{m(g-1)} \cos\alpha_{n+1} \cos\alpha_{n+2} \cdots \cos\alpha_g}{r_{m(n+1)} r_{m(n+2)} \cdots r_{m(g)} \cos\beta_n \cos\beta_{n+1} \ldots \cos\beta_{g-1}}, \\ B_{n|g} &= \frac{r'_{s(n)} r'_{s(n+1)} \cdots r'_{s(g-1)}}{r_{s(n+1)} r_{s(n+2)} \cdots r_{s(g)}}. \end{aligned} \tag{11}$$

Furthermore, the third-order ray aberrations on the image plane at a distance r'_0 from the optical element and perpendicular to the base ray OO_1 are derived,

$$\begin{aligned} x' = {} & d_{100}x + d_{200}x^2 + d_{020}y^2 + d_{300}x^3 + d_{120}xy^2 + d_{002}u^2 \\ & + d_{011}yu + d_{111}xyu + d_{102}xu^2, \end{aligned} \tag{12}$$

$$\begin{aligned} y' = {} & h_{010}y + h_{110}xy + h_{210}x^2y + h_{030}y^3 + h_{003}u^3 + h_{001}u \\ & + h_{101}xu + h_{201}x^2u + h_{021}y^2u + h_{012}yu^2, \end{aligned}$$

where the ray-aberration coefficients, d_{ijk} and h_{ijk}, are given by Lu & Zhu (2012).

In addition, similar to an axially symmetric optical system, the aberrations of a plane-symmetric optical system are related to l, the position of the pupil of each optical surface. The transfer equation of the pupil-position parameters is (Lu & Zhu, 2012)

$$l_{n+1} = \frac{1}{B_{n|n+1}^2}\, l_n + \frac{d_n}{B_{n|n+1}}. \tag{13}$$

where d_n is the distance from the nth element to the $(n+1)$th element.

4. Effect of second-order accuracy of aperture-ray coordinates and extrinsic aberrations

4.1. Transfer relationship of aperture-ray coordinates with second-order accuracy

Fig. 2 shows the optical scheme of an aperture ray $S_0P_1P_2$ passing through a double-element optical system. $S_0O_1O_2$ is the principle ray, $S_0P_1P_2$ is the aperture ray; the coordinate systems $x_iy_iz_i$, $x_{0(i)}y_{0(i)}z_{0(i)}$ and $x'_{0(i)}\,y'_{0(i)}\,z'_{0(i)}$ $(i = 1, 2)$ correspond to the optical surface, the entrance and exit wavefront, respectively. $x'_1\,y'_1\,z'_1$ is the coordinate system on the image

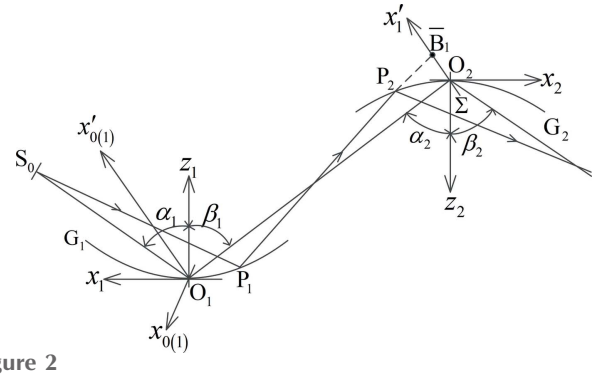

Figure 2
Optical scheme of an aperture ray $S_0P_1P_2$ passing through a double-element optical system.

plane Σ positioned at O_2, $\overline{B}_1$ is the intersection point of ray P_1P_2 and Σ.

The calculation of the total wave aberration requires the transformation of the aperture-ray coordinates of each element to the reference ones. As given in equation (10), the relation of the aperture-ray coordinates between adjacent optical surfaces adopts a linear approximation. However, for an XUV optical system with a small meridional curvature radius of the optical surface or a large field angle of a point source, if we also adopt the above transformation, it will result in inaccuracy of the wave aberration calculation. In this paper, we handle the transformation with the second-order polynomial of the aperture-ray coordinates between adjacent optical surfaces.

Since the field angle u is very small, the components containing only u are ignored in the derivation of the transfer relationship of the second-order accuracy of the aperture-ray coordinates on the optical surface. In order to obtain the relationship, we firstly need to know their transformation between the entrance wavefront and the optical surface. The expression of the second-order relation is

$$\begin{aligned} x_i &= \frac{1}{\cos\alpha_i}\, x_{0(i)} + 2\tan\alpha_i\, c_{0,2(i)}\, l_i\, y_{0(i)}\, u_i \\ &\quad + \frac{\sin\alpha_i}{\cos^3\alpha_i}\left(c_{2,0(i)} - \frac{\cos\alpha_i}{r_{\mathrm{m}(i)}}\right) x_{0(i)}^2 + \tan\alpha_i\, c_{0,2(i)}\, y_{0(i)}^2, \\ y_i &= \tan\alpha_i\left(1 - \frac{l_i}{r_{\mathrm{s}(i)}}\right) x_{0(i)}\, u_i + y_{0(i)} - \frac{\tan\alpha_i}{r_{\mathrm{s}(i)}}\, x_{0(i)}\, y_{0(i)}, \end{aligned} \tag{14}$$

where $x_{0(i)}$, $y_{0(i)}$, x_i, y_i are the aperture-ray coordinates on the entrance wavefront and the optical surface of the ith element, respectively.

Then, we can calculate the ray coordinate on the image plane Σ that lies in the position of the entrance wavefront of the $(i+1)$th element using the aperture-ray coordinates on the optical surface of the ith element, x_i, y_i,

$$\begin{aligned} x_i' &= P_{100(i)}\, x_i + P_{011(i)}\, u_i\, y_i + P_{200(i)}\, x_i^2 + P_{020(i)}\, y_i^2, \\ y_i' &= T_{101(i)}\, x_i\, u_i + T_{010(i)}\, y_i + T_{110(i)}\, x_i\, y_i, \end{aligned} \tag{15}$$

where the expressions for coefficients $P_{klm(i)}$ and $T_{klm(i)}$ are given by

$$\begin{aligned} &P_{100(i)} = \Lambda_{\mathrm{m}(i)}\cos\beta_i, \quad P_{011(i)} = -2\Lambda_{\mathrm{m}(i)} c_{0,2(i)}\, l_i \sin\beta_i, \\ &P_{200(i)} = \Lambda_{\mathrm{m}(i)}\left(\frac{\cos\beta_i}{r'_{\mathrm{m}i}} - c_{2,0(i)}\right)\sin\beta_i, \\ &P_{020(i)} = -\Lambda_{\mathrm{m}(i)} c_{0,2(i)} \sin\beta_i, \quad T_{101(i)} = \Lambda_{\mathrm{s}(i)}\Lambda'_{l(i)}\sin\beta_i, \\ &T_{010(i)} = \Lambda_{\mathrm{s}(i)}, \quad T_{110(i)} = \frac{\Lambda_{\mathrm{s}(i)}\sin\beta_i}{r'_{\mathrm{s}i}}, \end{aligned} \tag{16}$$

with $\Lambda_{\mathrm{m}(i)} = 1 - r_0'/r'_{\mathrm{m}(i)}$, $\Lambda_{\mathrm{s}(i)} = 1 - r_0'/r'_{\mathrm{s}(i)}$, $\Lambda'_{l(i)} = 1 + l_i/r'_{\mathrm{s}(i)}$; in addition, $r_0' = d$ in equation (15), and d_i is the distance between the ith element and the $(i+1)$th element.

From Fig. 2, the coordinates x_i', y_i' should be transformed into the coordinate system of the entrance wavefront of the $(i+1)$th element, $x_{0(i+1)}y_{0(i+1)}z_{0(i+1)}$; the transformation relation is

$$\begin{aligned} x_{0(i+1)} &= -x_i', \\ y_{0(i+1)} &= y_i'. \end{aligned} \tag{17}$$

We then apply equation (17) to obtain the aperture-ray coordinates on the optical surface of the $(i+1)$th element, x_{i+1}, y_{i+1}. Consequently, combining equations (14)–(17), the relation of the aperture-ray coordinates on the optical surface of the second-order accuracy between the ith and $(i+1)$th element can be obtained,

$$\begin{aligned} x_2 &= \frac{1}{A_1}x_1 + 2\phi_1 u_1 y_1 + \frac{\phi_2}{A_1}x_1^2 + \phi_3 y_1^2, \\ y_2 &= -\frac{1}{B_1}y_1 + \phi_4 u_1 x_1 + \frac{\phi_5}{r'_{\mathrm{s}1}}x_1 y_1, \end{aligned} \tag{18}$$

where

$$\phi_1 = c_{0,2(2)}\, l_2 \tan\alpha_2 - \frac{c_{0,2(1)}\, l_1 \tan\beta_1}{A_1}, \tag{19}$$

$$\phi_2 = \frac{c_{2,0(2)}\tan\alpha_2}{A_1} - c_{2,0(1)}\tan\beta_1 + \frac{\sin(\beta_1 - \alpha_2)}{r'_{\mathrm{m}1}\cos\alpha_2}, \tag{20}$$

$$\phi_3 = \frac{c_{0,2(2)}\tan\alpha_2}{B_1^2} - \frac{c_{0,2(1)}\tan\beta_1}{A_1}, \tag{21}$$

$$\phi_4 = -\left(\frac{\sin\beta_1}{B_1}\Lambda'_{\mathrm{s}(1)} + \frac{B_1\sin\alpha_2}{A_1}\Lambda_{\mathrm{s}(2)}\right), \tag{22}$$

$$\phi_5 = \frac{\sin\alpha_2}{A_1} - \frac{\sin\beta_1}{B_1}. \tag{23}$$

4.2. Extrinsic aberrations

The definition of the intrinsic wave aberration is based on a model of a single optical surface with the assumption of an ideal point object. However, for a multi-element optical system, the assumption of an ideal point object, to some optical surface of the optical system (except the first one), is no longer valid because of the effect of aberrations of its preceding ones. Taking this into account, the resultant change of aberration is regarded as extrinsic aberrations. Therefore, the actual total aberration of the optical systems comprises intrinsic aberrations and extrinsic aberrations (Sasian & Acosta, 2014; Sasian, 2013; Lu & Cao, 2017).

Fig. 3 shows an optical system of two optical surfaces G_1 and G_2; $x_1'\,O_1'\,y_1'$ is the coordinate system of image plane Σ_1' at a distance r_0^* from optical surface G_1. The coordinates of B_1 are determined by the second-order accuracy of the aperture-ray coordinates, and those of B_1' also include the effect of the extrinsic aberration.

According to the third-order aberration calculation expressions of a plane-symmetric optical system, the aberrations on the image plane positioned at G_2 (*i.e.* in the case of $r_0^* = d$ in Fig. 3) are calculated by

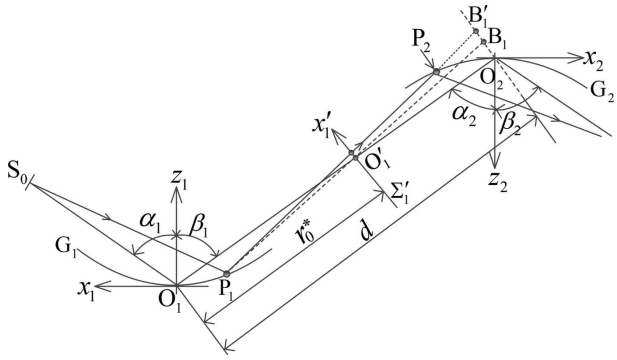

Figure 3
Optical system of two optical surfaces G_1 and G_2. B_1 and B_1' represent the aperture-ray coordinates on G_2 with and without the extrinsic aberration, respectively.

$$\Delta x_1' = \frac{3dw_{300(1)}\,x_1^2}{\cos\beta_1} + \frac{dw_{120(1)}\,y_1^2}{\cos\beta_1} + \frac{dw_{111(1)}\,u_1\,y_1}{\cos\beta_1} - \frac{dw_{102(1)}\,u_1^2}{\cos\beta_1},$$
$$\Delta y_1' = dw_{111(1)}\,u_1\,x_1 + 2dw_{120(1)}\,x_1\,y_1. \tag{24}$$

Therefore, the aberrations will cause the aperture-ray coordinates on the optical surface of G_2 to change by the amount

$$\Delta x_2 = -\frac{\Delta x_1'}{\cos\alpha_2}, \qquad \Delta y_2 = \Delta y_1'. \tag{25}$$

4.3. Modification of aberrations of a double-element optical system with the second-order accuracy of the aperture ray and extrinsic aberrations

According to the above discussions, the actual aperture-ray coordinates on the optical surface of G_2 should be

$$\begin{aligned} X_2 &= x_2 + \Delta x_2 \\ &= \frac{1}{A_1}x_1 + \left(2\phi_1 - \frac{dw_{111(1)}}{\cos\beta_1\cos\alpha_2}\right)y_1u_1 \\ &\quad + \left(\frac{\phi_2}{A_1} - \frac{3dw_{300(1)}}{\cos\beta_1\cos\alpha_2}\right)x_1^2 + \left(\phi_3 - \frac{dw_{120(1)}}{\cos\beta_1\cos\alpha_2}\right)y_1^2 \\ &\quad - \frac{dw_{102(1)}}{\cos\beta_1\cos\alpha_2}u_1^2, \end{aligned} \tag{26}$$

$$\begin{aligned} Y_2 &= y_2 + \Delta y_2 \\ &= -\frac{1}{B_1}y_1 + (\phi_4 + dw_{111(1)})x_1u_1 + \left(\frac{\phi_5}{r_{s1}'} + 2dw_{120(1)}\right)x_1y_1. \end{aligned}$$

Obviously, the first term of the right-hand side of equation (26) represents the linear approximation of the aperture-ray coordinates.

Therefore, the actual wave aberration of a double-element optical system is given by

$$W_T = W_{(1)} + W_{(2)}, \tag{27}$$

where the calculation expressions of $W_{(1)}$ and $W_{(2)}$ are

$$\begin{aligned} W_{(1)} &= \sum_{ijk}^{4} w_{ijk(1)}\,x_1\,y_1\,u_1, \\ W_{(2)} &= \sum_{ijk}^{4} w_{ijk(2)}\,X_2\,Y_2\,u_2. \end{aligned} \tag{28}$$

In Section 3, the aberration expressions of equation (12) use x_2, y_2, u_2 as the aperture-ray coordinates and the field angle. Therefore, the contribution of aberrations caused by the wave aberrations of G_1 should use x_2, y_2, u_2 to calculate; and, according to equation (26), the actual aperture-ray coordinates and the field angle of the aberrations calculation of G_2 should adopt X_2, Y_2, u_2.

According to the above discussions, expressions of the actual aberration coefficients can be obtained. For the convenience of the aberration calculation, the calculation of the aperture-ray coordinates of the aberrations in the case of the linear approximation uses x_2, y_2, u_2; in the remaining cases, x_1, y_1, u_1 are used to calculate the aberration. Therefore, they are given by

$$\begin{aligned} x_2' &= \sum_{ijk}^{4}\left(d_{ijk}\,x_2^i\,y_2^j\,u_2^k + \tilde{d}_{ijk}\,x_1^i\,y_1^j\,u_1^k\right), \\ y_2' &= \sum_{ijk}^{4}\left(h_{ijk}\,x_2^i\,y_2^j\,u_2^k + \tilde{h}_{ijk}\,x_1^i\,y_1^j\,u_1^k\right), \end{aligned} \tag{29}$$

where the first parts of the right-hand sides of each equation, d_{ijk} and h_{ijk}, are just the aberrations coefficients obtained with the linear approximation of the aperture ray; the second parts result from the total of the modification coefficients of the aberrations due to the second-order accuracy of the aperture-ray coordinates, and the extrinsic aberrations coefficients, $\tilde{d}_{ijk}$ and $\tilde{h}_{ijk}$, are given in the supporting information.

5. Numerical validation

To validate the aberration formulae derived above, we now apply them to calculate the imaging of two design examples of an XUV optical system and compare them with the ray-tracing results from the *SHADOW* software. Optical system I is the Tondello's spectrograph: a spherical-grating monochromator with a pre-focusing toroidal mirror, as shown in Fig. 4. The optical system accepts from the source a light beam with a diverging angle of $2\theta_v \times 2\theta_h$ = 10 mrad × 20 mrad; the monochromator uses a conventional spherical grating with a groove density of N = 600 grooves mm^{-1}, and works in a +1 diffraction order at a wavelength of 4.4 nm. Its other optical parameters are listed in Table 1.

Optical system II is a modified design of optical system I. The optical parameters to be modified are the major and minor curvature radius of the toroidal mirror, R_1 = 4300 cm, ρ_1 = 25 cm; and its other optical parameters are consistent with that of optical system I. Using these optical parameters, we can obtain r_{m2}' = 119.35 cm, r_{s2}' = 79.81 cm.

Fig. 5 shows ray spot diagrams of optical system I with an image distance of r_0' = 150 cm: parts (*a*) show the calculation

Table 1
Optical parameters of optical system I [units: cm (unless otherwise stated)].

r_{m1} (r_{s1})	θ_1	R_1	ρ_1	d	R_2	α_2	β_2	r'_{m2}	r'_{s2}
358.39	86°	4151.33	27	277.84	1000	−88°	85.38°	80.55	140.56

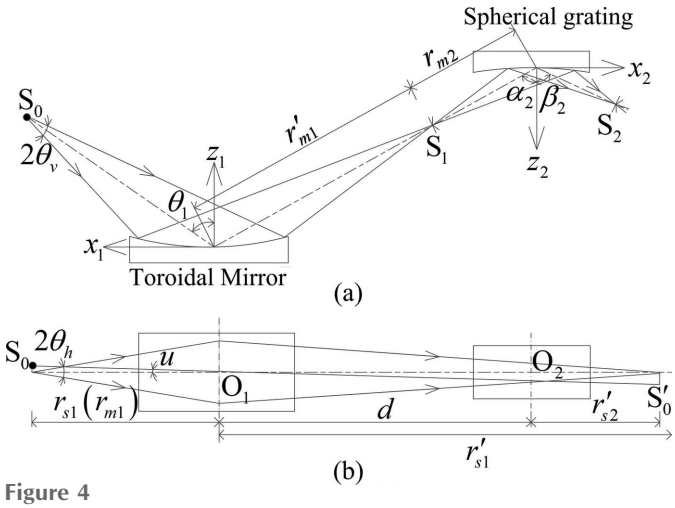

Figure 4
Optical scheme of optical system I.

results using the aberration coefficients of the first term of equation (29), d_{ijk}, h_{ijk}; parts (*b*) use the total aberration coefficients of equation (29), d_{ijk} and $\tilde{d}_{ijk}$, h_{ijk} and $\tilde{h}_{ijk}$; and parts (*c*) show the ray-tracing results from *SHADOW*. In the spot diagrams (I), (II) and (III), point sources with field angles of $u_1 = 0°$, 0.1° and 0.2°, respectively, are assumed.

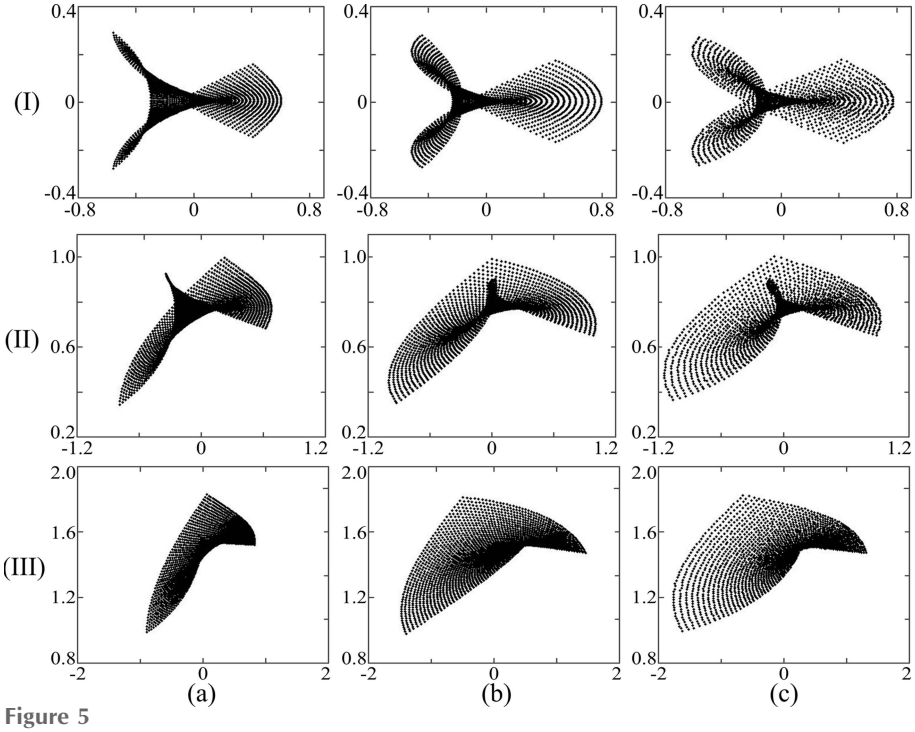

Figure 5
Ray spot diagrams for an optical system with an image distance of $r'_0 = 150$ cm (axis units: cm). Ray spot diagram (*a*) is obtained with the aberration coefficients d_{ijk}, h_{ijk}; (*b*) with d_{ijk} and $\tilde{d}_{ijk}$, h_{ijk} and $\tilde{h}_{ijk}$; and (*c*) with ray-tracing program *SHADOW*. (I), (II) and (III) are for point sources with field angles of $u_1 = 0°$, 0.1° and 0.2°, respectively.

Fig. 6 shows the ray spot diagrams of optical system II. Ray spot diagrams (*a*), (*b*) and (*c*) are obtained in the same way as in (*a*), (*b*) and (*c*) of Fig. 5. Here, (I) is for a point source with a field angle of $u_1 = 0°$ and an image distance of $r'_0 = 119.35$ cm; (II) and (III) are for point sources with field angles of $u_1 = 0.1°$ and $u_1 = 0.2°$ and an image distance $r'_0 = 200$ cm.

As shown in Figs. 5 and 6, the results of aberrations obtained with d_{ijk}, h_{ijk} are unacceptable, but the aberration calculation accuracy obtained with d_{ijk} and $\tilde{d}_{ijk}$, h_{ijk} and $\tilde{h}_{ijk}$ are satisfactory compared with the ray-tracing results. The difference is yielded by the contribution of the high-order aberrations and high-order coordinate components in the transfer of the aperture ray; but, for a source of dimension ~1 mm, like a synchrotron radiation light source or laser, the contribution of the high-order aberrations and the effect of aberrations due to the high-order coordinate components in the transfer of the aperture ray can be negligible; and thus the aberration expressions derived in this paper have a satisfactory calculation accuracy.

6. Conclusions

In this paper we propose a calculation method of the effect on the aberrations due to the second-order accuracy of aperture-ray coordinates and the extrinsic aberrations based on the third-order aberration theory of plane-symmetric optical systems, and derive their calculation expressions.

The resultant aberration formulae are applied to calculate the imaging of two design examples of XUV optical systems to compare their results with those obtained from the ray-tracing program *SHADOW*, and they have a satisfactory calculation accuracy.

Compared with the *SHADOW* software, the method proposed in this paper can analyze the contribution of different types of aberrations, the relationship between the optical parameters and the aberrations, *etc.* Therefore, it will provide an analytical measure and will be helpful in the design and optimization of XUV multi-element optical systems.

Acknowledgements

The authors gratefully appreciate Professor Lijun Lu from Shanghai University for helpful discussions and useful comments.

Funding information

The following funding is acknowledged: Project from Fujian Provincial Depart-

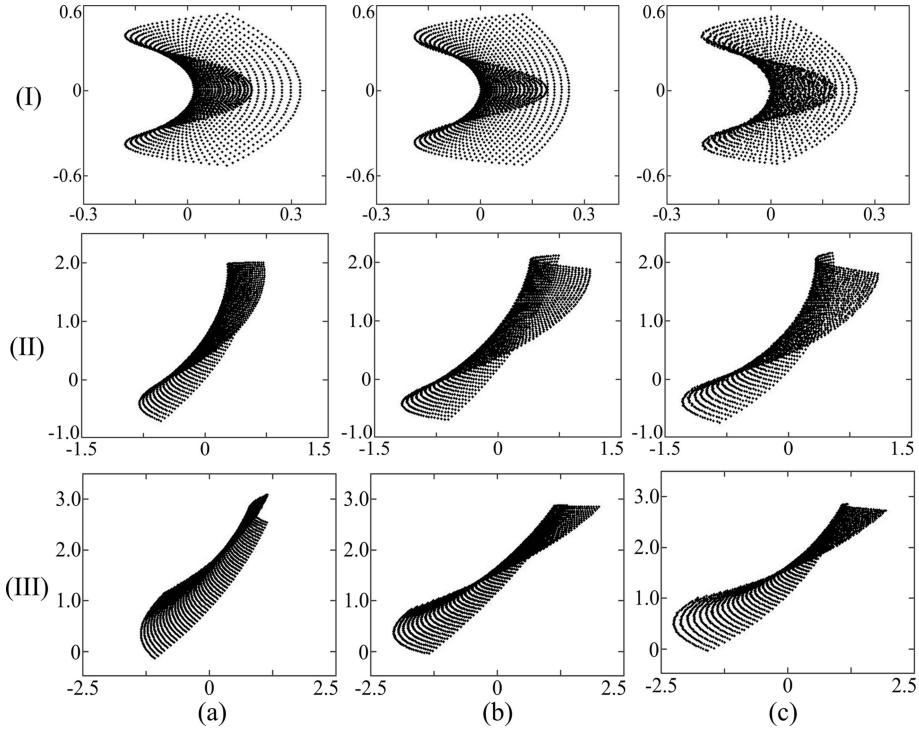

Figure 6
Ray spot diagrams for optical system II. Ray spot diagrams (*a*), (*b*) and (*c*) are obtained in the same way as (*a*), (*b*) and (*c*) of Fig. 5; (I) is for the point source with field angle of $u_1 = 0^\circ$ and image distance of $r_0' = 119.35$ cm; (II) and (III) are for point sources with field angles of $u_1 = 0.1^\circ$, $u_1 = 0.2^\circ$ and image distance $r_0' = 200$ cm, respectively.

ment of Science and Technology of China (grant No. 2017H0032); Introduction of Talent Research Start-up Fee Project of Putian University (grant No. 2019010).

References

Beulter, H. G. (1945). *J. Opt. Soc. Am.* **35**, 311–350.
Cao, Y. Q. & Lu, L. J. (2017). *J. Opt. Soc. Am. A*, **34**, 299–307.
Chrisp, M. P. (1983). *Appl. Opt.* **22**, 1508–1518.
Goto, K. & Kurosaki, T. (1993). *J. Opt. Soc. Am. A*, **10**, 452–465.
Lu, L.-J. (2008). *J. Synchrotron Rad.* **15**, 399–410.
Lu, L. J. & Cao, Y. Q. (2017). *Appl. Opt.* **56**, 8570–8583.
Lu, L. J. & Lin, D. L. (2010). *Optik*, **121**, 1198–1218.
Lu, L. J. & Zhu, G. Q. (2012). *Optik*, **123**, 157–166.
Masui, S. & Namioka, T. (1999). *J. Opt. Soc. Am. A*, **16**, 2253–2268.
Namioka, T., Koike, M. & Content, D. (1994). *Appl. Opt.* **33**, 7261–7274.
Noda, H., Namioka, T. & Seya, M. (1974). *J. Opt. Soc. Am.* **64**, 1031–1036.
Owen, R. L., Juanhuix, J. & Fuchs, M. (2016). *Arch. Biochem. Biophys.* **602**, 21–31.
Palmer, C., McKinney, W. & Wheeler, B. (1998*a*). *Proc. SPIE*, **3450**, 55–66.
Palmer, C., Wheeler, B. & McKinney, W. (1998*b*). *Proc. SPIE*, **3450**, 67–77.
Peatman, W. B. (1997). *Gratings, Mirrors and Slits: Beamline Design for Soft X-ray Synchrotron Radiation Sources*, pp. 71–75. Amsterdam: Gordon and Beach.
Sanchez del Rio, M., Canestrari, N., Jiang, F. & Cerrina, F. (2011). *J. Synchrotron Rad.* **18**, 708–716.
Sasian, J. (2013). *Adv. Opt. Technol.* **2**, 75–80.
Sasian, J. & Acosta, E. (2014). *Opt. Express*, **22**, 289–294.
Shealy, D. L., Wang, C. & Hoover, R. B. (1995). *J. X-ray Sci. Technol.* **5**, 1–19.
Underwood, H. J. & Koch, J. A. (1997). *Appl. Opt.* **36**, 4913–4921.
Yang, F. G., Li, M., Gao, L. D., Sheng, W. F., Liu, P. & Zhang, X. W. (2016). *Opt. Lett.* **41**, 2815–2818.